Journal of Civil Structural Health Monitoring
https://doi.org/10.1007/s13349-024-00794-w

ORIGINAL PAPER

Structural health monitoring of an onshore steel wind turbine

Marco Simoncelli[1] · **Marco Zucca**[2] · **Matteo Ghilardi**[3]

Received: 20 June 2023 / Accepted: 12 March 2024

Abstract
The study presents the development of a structural monitoring system installed in a 45-m-high steel wind tower located in Italy. The installed monitoring system was composed by 16 strain gauges placed in the tower wall, in a pattern of four Wheatstone bridges at 45°, together with thermal couples, at 21 m from the ground (half-height of the tower). Moreover, several accelerometers were placed along the tower height (with one of them located next to the strain gauges). The wind velocity and directions were obtained directly from the turbine own monitoring system. Such a monitoring system was designed because, due to the decrement of the total height from the original design, the tower suffers from resonance problems. In fact, the investigated tower was originally designed with 65 m of height but then, to comply with local regulations, the height was decreased to the actual size. Therefore, to allow safe operation and avoid excessive fatigue due to the increased displacements, the velocity of the rotor has been manually limited causing an important reduction in the energy production. The results of the study show the importance of monitoring the resonance issue. The differences between the damage indexes obtained with two different working conditions are discussed: tower working with limited operational capacity and tower working at its maximum capacity (in resonance).

Keywords Steel wind turbine · Fatigue checks · Continuous monitoring · Strain-gauges · Resonance

1 Introduction

The extensive use of fuel in the last century led the new generation into a deep energetic crisis. Climate change and environmental degradation are a huge threat to Europe and worldwide. To overcome these challenges, the European Green Deal was developed with the main aim to promote the efficient use of resources by moving towards a clean and circular economy [1–3]. Moreover, the events that occurred over the last three years (lockdown due to COVID-19, war, etc.) stressed the need for each European country to become as much energetic independent as possible. An important step can be taken towards producing electricity from renewable sources: this is the topic on which a good portion of modern scientific research is focusing [4]. In this direction, obtaining electricity by exploiting the natural wind force represents an excellent eco-sustainable and very profitable solution. The well-known wind farms have been widely installed over the last thirty years. Wind farms consist of wind towers (Fig. 1), which are vertical structures generally made of steel or concrete and used to elevate turbines (and blades) to a designed height. Due to the increase in energy production, the shape of the blades can highly vary from one tower to another, also involving new and innovative materials in their fabrication [5]. Of course, the total tower height is of paramount importance as well and can be directly related to the energy produced. Indeed, this is what the modern engineering competition is about: designing a tall and slender tower that can both withstand, throughout its service life, all the dynamic actions due to wind and the motion of the turbine itself and produce as much electricity as possible [6–8].

Different types of wind towers are marketed, which can be placed on land (onshore) or in the open sea (offshore); onshore steel turbines are generally realised using a tubular steel column with different diameters along the height (Fig. 2), whereas, in the case of offshore structures, a lattice

✉ Marco Simoncelli
marco.simoncelli@polimi.it

[1] Department of Architecture, Built Environment and Construction Engineering, Politecnico di Milano, Milan, Italy

[2] Department of Civil, Environmental and Architecture Engineering, University of Cagliari, Cagliari, Italy

[3] Seva SRL, Milan, Italy

Published online: 11 April 2024

Fig. 1 Example of a wind farm (www.sevasrl.it)

Fig. 2 A tubular steel tower and its main components

trussed or mixed lattice-tubular columns are used. 2020 was a record year for global wind power despite the COVID-19 pandemic: the total cumulative installed electricity generation capacity from wind turbines reached 743GW. Since the offset of the third millennium up to now, the electricity generation capacity has increased up to 50 times [9].

For the design of these huge structures, a high-level engineering knowledge is required; nevertheless, collapses due to wrong design or poor maintenance are quite common [10, 11]. Recent publications have shown that collapses are mainly due to huge fires caused by electrical problems on rotors, insufficient bolt strength, poor bolt quality control during construction or collapse of the connections due to maximum fatigue life [12]. Moreover, the rotor-steel turbine resonance can also generate vast and dangerous displacements that can yield a global collapse [13]. The problem of fatigue is even more complicated than in the classic steel industrial buildings, as wind towers are not stationary structures and hence fatigue design must consider all their peculiarities. From a structural point of view, a wind tower can be simplified as a cantilever beam, with a variable cross section along its length and an eccentric mass concentrated at the free end. Also, the interaction with the soil should be always considered by using ad-hoc calibrated springs or by modelling the soil itself with finite (FEM) *brick/shell* elements. The design of these structures is performed by adequately mixing the use of the various packages of finite element software with the equations deriving from design practice and prescribed in the standards. Finite element analyses can be used in different degrees of

detail: the *beam* elements are usually used for the global behaviour, whereas the connections, the foundations and the presence of openings require more advanced FEM elements, like *shell* and *brick*. According to IEC61400 [14], these structures should be designed considering two safety classes: (i) *normal safety class* when the failure is directly related to injury with economic and social consequences; and (ii) *special safety class* when the safety requirements are agreed between manufacturer and customer. Main loads acting on onshore structures are the structural self-weight, the weight of the rotor acting at the top of the tower, the accumulation of ice, the wind action and any operational loads. Normally, wind could be evaluated using Eurocode 1 [15], considering both the resonance problem and the pressure; for more advanced evaluations, advanced Computational Fluid Dynamics (CFD) software could be used [16]. An accurate analysis of the tower should consider the time history of the wind acting in time. The seismic action must be considered in zones typically affected by strong earthquakes [17]. A methodology for seismic risk assessment of steel turbines is presented in [18] deriving fragility curves from an incremental dynamic approach by considering the buckling and the residual tilt. Other rare conditions (extreme loads) can occur, like accidental actions, explosions and lightning. It should be remarked that one of the key aspects in the design of the support structure is avoiding oscillations in resonance when the tower is excited by variations in the rotor load [13]. The overall damping ratio can be assumed about 3% for longitudinal oscillations (fore-aft, out of rotor plane), whereas it is an order of magnitude lower in the case of the transverse motion (side to side, in rotor plane). When the frequencies of the rotor coincide with (or are very close to) the natural ones of the structure, unacceptable deformations would be reached. To prevent massive structural damage, the integrated control system of the wind turbine continuously monitors the displacements and the accelerations on the top of the tower and automatically performs a shutdown if a predetermined threshold is exceeded. It should be noted that in wind turbines frequencies always depend on the foundation soil and their interaction with the structure since the foundations consist of extremely huge and important concrete structures. The DNVGL-ST-0126 standard [19] prescribes that the fundamental mode of vibrating maintains an estimated safety margin of 5% with respect to the operating frequencies of the rotor.

In general, steel turbines are designed to have a 20-year service life before being dismantled, producing enormous environmental issues. Some authors proposed very clever and interesting solutions to reuse the waste steel coming from dismantled turbines [20]; however, these do not consider the reuse of foundations, which are huge reinforced concrete blocks that cannot be easily removed from the ground (Fig. 3).

To overcome the *pollution* problem, an efficient solution lies in expanding the service life of the tower itself; to this aim, structural designers and standards should focus more on increasing the performance of parts and components, such as connections. On the other hand, constructors should improve quality controls and maintenance. In this context, a permanent structural health monitoring system based on the use of strain-gauges, thermal couples, anemometers and accelerometers can grant a constant assessment of the turbine's condition. Such monitoring systems can check daily the status of the tower and predict the residual life of the component being monitored, preventing local damages and hence global failure. Unfortunately, such a system is not common, as the dimensions of turbines actually make it very hard to install instrumentation on existing towers [21]. In [22] the results of 2-years dynamic monitoring of a 5 MW wind turbine are presented, with a focus on the resonance phenomena. In 2011 [23] strain-gauges were used to monitor crack propagation on connections of a small wind tower in Italy. Moreover, in the context of an important European project, a real-scale wind turbine was monitored, whose results were used

Fig. 3 Typical wind turbine foundation in reinforced concrete

to develop a correct estimation of the connections' fatigue life [24, 25]. The study of the response in terms of modal shapes and frequencies can also directly inform on the state of damage of the turbine itself. In references [26, 27] the importance of the use of such expensive and complex structural monitoring system is presented, which can reveal the damaged situation of the components in real-time, as well as any modification of modal shapes due to damage.

In this research, a 45 m tower located in Italy [13] has been continuously monitored for 1 year: 16 strain gauges were placed in a pattern of four Wheatstone bridges at 45°, together with thermal couples, at a specific elevation level (21 m of height). The monitoring system worked with a remote acquisition board accessible online and remotely; different operational conditions were tested. The wind velocity and direction were always registered via the control system of the turbine itself. In addition, several accelerometers were placed along the tower height, having one of them in the same section equipped with strain gauges.

The turbine starts operating when the wind velocity overpasses 3 m/s with a specific limit on the nacelle speed. In fact, at a velocity greater than 30 rpm the tower starts to exhibit big top displacements (due to a resonance problem highlighted by the installed accelerometers) and, when 32 rpm are reached, the emergency system shuts down the turbine and hence energy production. This paper aims to show the stresses experimentally measured in normal operating condition and at the maximum permitted rotor velocity, in resonance (32 rpm). Moreover, stresses were directly used to evaluate a damage index (D_d) based on the Palmgren–Miner rule. The advantages and issues associated with the use of the monitoring system are discussed.

2 Remarks on the fatigue problem

Steel towers are divided into multiple tubular steel pieces that could be easily carried in situ. Generally, these pieces feature a huge diameter and a reduced thickness. From a design standpoint, these profiles (belonging to class 4 of EC3-1-1 [28]) consist of slender plates in which local buckling phenomena occur if a compression state exists (caused by pure compression or bending). Therefore, the cross-section can neither rely on plasticity nor reach the elastic resistance limit. In all the structural safety checks, the cross-section properties used in the verification equations (i.e. gross area and section moduli) must be reduced by evaluating the effective properties (effective area and effective section elastic moduli). These pieces are generally connected with ring flanges using high-strength preloaded bolts (Fig. 4): this is why granting the rig's flatness is of paramount importance. Imperfections on the flanges cause loss of contact between each other, leading to water ingress and consequent bolt corrosion. Shell sections near flanges, bolts and welded details are subjected to high cyclic loads with considerable numbers of load cycles and variable amplitudes. Moreover, due to the high-notch effect of the thread, bolts are extremely susceptible to fatigue damage. Several European projects were developed over the last years with the aim of improve the fatigue life of the connections. In particular, within the framework of HISTWIN, HISTWIN2 and SHOWTIME projects, included in the RFCS research programme [25], an innovative friction connection was proposed. The comparison between the *proposed* and *classic* connections showed a similar value in terms of initial stiffness and a slightly different ultimate resistance. Main advantages of using the developed solution are, no prying forces acting on the connection and no presence of welding. These improvements increase the fatigue life of the connections and, consequently, of the tower.

It is universally acknowledged that the best way to represent the effects of the loads acting on a cross-section or at some point of the structure is to use the time-history (or time-series) analysis, as in the case of fatigue checks of steel components it produces highly reliable results. A time-history analysis holds all the information that is needed for the fatigue design. To use data from irregular load histories for practical fatigue design, the number of cycles (i.e. their counting) must be extracted [29]. One of the most used methods—and the one considered in this work—is known as *Rainflow*. The *Rainflow* algorithm

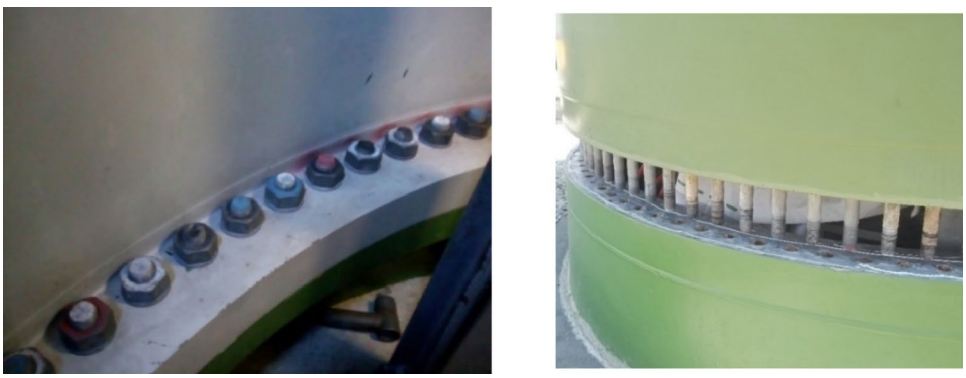

Fig. 4 Typical flange-to-flange connection with high-strength preloaded bolts

used for half-cycle counting is the one available online for free written in MATLAB language [30].

The Palmgren–Miner approach can be suitably used to perform a fatigue evaluation. The result of a fatigue design is the Wöhler curve (or S/N curve) which relates the load range and the number of cycles (Fig. 5). In this way, each of the design load cases requiring fatigue design is simulated producing a set of time-series. The spectrum should be estimated experimentally or should be given by the wind turbine manufacturer, which is generally from the safe side.

A common practice in use by steel turbine designers consists of a further simplification in the fatigue loading by relying on the Damage Equivalent Loads (DEL); the DEL is the equivalent load (or load effect) with constant amplitude that would produce the same damage in the structure as the damage induced by the original time series of the same load (Fig. 5). The passages from the knowledge of the stresses' variation, Ds, to the equivalent one, $Ds_{E,ref}$, is based on Eq. (1):

$$\mathrm{DEL} = \Delta\sigma_{E,\mathrm{ref}} = \left(\sum \frac{n_i \Delta\sigma_i^m}{N_{\mathrm{ref}}}\right)^{\frac{1}{m}} \tag{1}$$

where m is the slope of the Wöhler curve; n_i is the number of cycles corresponding to load range $\Delta\sigma_i$ in the original time history and N_{ref} is the reference number of cycles for which the reference DEL is evaluated. A typical S–N curve for steel structures has two different Wöhler slopes, $m=3$ and $m=5$. In principle, the DEL will include load cycles acting in the range of both Wöhler slopes and therefore the standard Wöhler slope cannot be used. For steel, common values are $m=4$ and $N_{\mathrm{ref}}=2\times10^6$.

Subsequently, the fatigue check can be evaluated via the following equation:

$$\gamma_{\mathrm{Ff}}\Delta\sigma_{E,\mathrm{ref}} \le \sqrt[m]{D_{\mathrm{d}}}\frac{\Delta\sigma_{\mathrm{c}}}{\gamma_{\mathrm{Mf}}} \text{ or } \frac{\Delta\sigma_{E,\mathrm{ref}}}{\frac{\Delta\sigma_{\mathrm{c}}}{1.1}} \le 1 \tag{2a, b}$$

where D_{d} is the damage of the structure (1 is the maximum admissible), $\Delta\sigma_{\mathrm{c}}$ is the detail category according to EC3-1-9

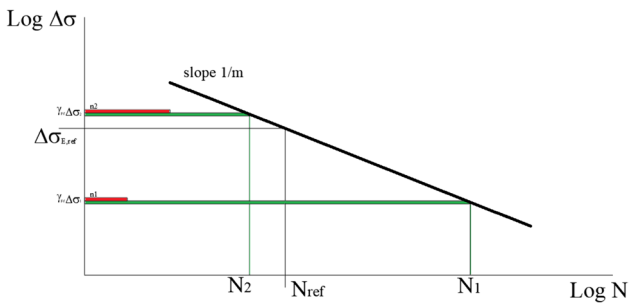

Fig. 5 Example of DEL evaluation (Eq. 1)

and γ_{Ff} and γ_{Mf} are safety factors taken as 1.00 and 1.10, respectively.

3 The monitoring system

A monitoring system is always embedded in all the installed wind turbines, running under the responsibility of the tower's owner. Connecting the acquisition board with the existing system allowed wind velocity and direction, rotor velocity and pitch angle to be continuously registered.

3.1 Description of the structure and the monitoring system

The wind turbine under consideration was initially designed with a total height of 65 m. However, due to Italian law prescriptions for landscape preservation, it was assembled with a total hub height of almost 45 m. The turbine is equipped with a main shaft that directly connects the generator to the rotor hub mounting three blades (Fig. 6). The blades' diameter is about 40 m. The wind turbine does not rely on any system for reducing the number of revolutions and is equipped with a crankshaft that directly connects the generator to the propeller rotor consisting of three blades. The asynchronous generator grants a variable number of revolutions and its diameter is 2.5 m. Maximum power at the maximum rotation speed is approximately 500 kW. The foundation consists of a single huge reinforced concrete cylinder (diameter: 13 m; height: 3 m) plus 16 concrete piles (diameter: 0.8 m; length: 10 m). A tubular piece of steel has been embedded inside the concrete foundation and then connected to the first tubular piece using a ring flange. The geometrical details of the turbine are shown in Fig. 7 and Table 1; all the connections were realised using welded ring flanges with preloaded high-strength bolts like the ones shown in Fig. 4. Due to the high diameter/thickness ratio of the cross-sections, the effective area and effective section elastic moduli have been evaluated, via the iterative procedure described in the HISTWIN European project [25].

Despite structural checks met the limits of the Eurocode, once the shaft rotation value becomes greater than 30 rpm (operational rotation condition to guarantee a satisfactory level of energy production), the tower starts to show severe oscillations that trigger the safety systems (shutdown) based on the output of the instruments installed on the hub. To understand the nature of the problem an experimental campaign by means of several PCB393A03 type accelerometers (sensitivity 1000 mv/g, range ± 5 g) installed along the tower height in different locations, as shown in Fig. 6, was conducted. As deeply discussed in Ref. [13], it has been assessed that the oscillations were independent of the environmental conditions, and it was mainly due to a structural

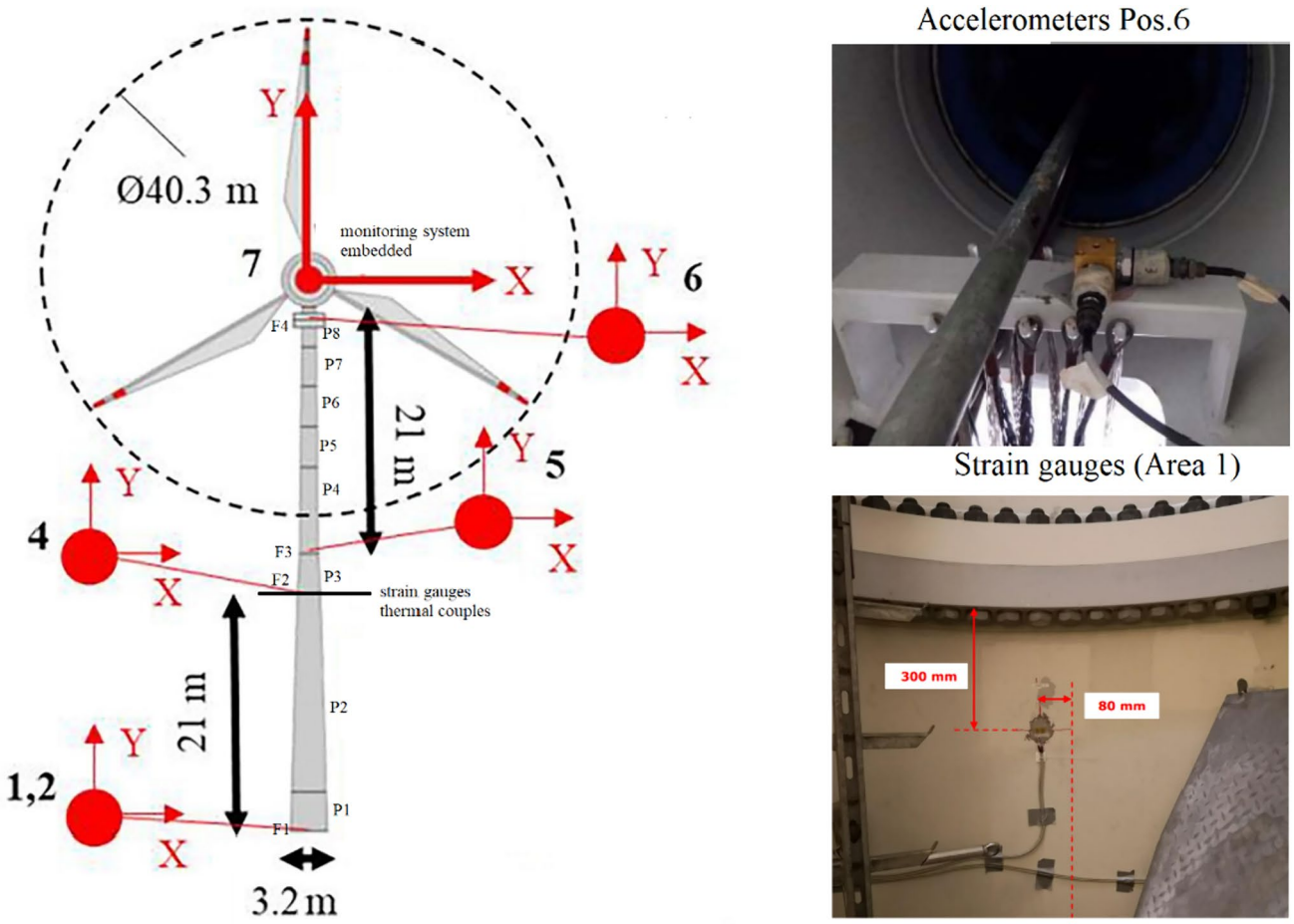

Fig. 6 The monitored tower with the position of the instruments

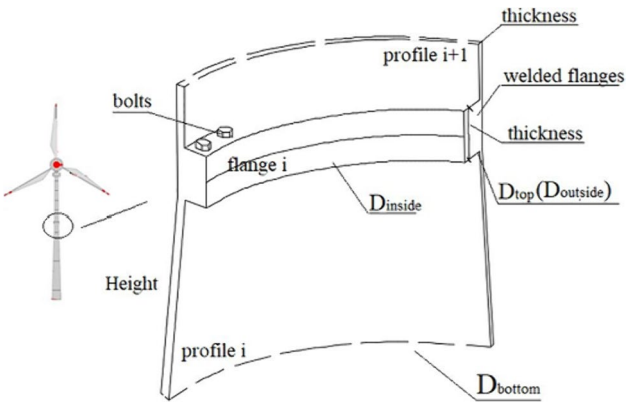

Fig. 7 Main parts of the tower described in Table 1

resonance issue. In particular, the first fundamental mode of the turbine (almost 0.6 Hz) was exactly the operation frequency of the rotor, which thus led to a resonance problem. To guarantee the service life of the tower an operational limit has been set to the rotor.

To understand the influence of this resonance problem on the internal stresses a second monitoring system was installed. In particular, a total of 16 strain gauges (350 Ω, gauge factor 1.5) have been placed at the end of P2 next to flange F2 (21 m from the ground) in a pattern of four Wheatstone bridges at 45° spacing. Each one has been obtained by connecting four strain gauges in a full-bridge configuration. The bridge unbalance, which is caused by the varying bending loads in the tower, can be directly related to the shell deformation once the gauge factor and the input voltage are known. The tower section selected for monitoring is located close to the intermediate flanged connection, at about 21 m height from the ground. The presence of a resting platform made this a suitable spot. In addition, four thermal couples were mounted to monitor the structural steel temperature (Fig. 8). This allows for considering the thermic delta and correcting the readings accordingly. The installation of the strain gauges was performed by specialised technicians. First coating was removed and the steel cleaned properly. Due to temperatures dropping near zero, a heat gun had to be used prior to

Table 1 Details of the main parts of the tower

	Height (m)	D_{bottom} (mm)	D_{top} (mm)	Flange (n°)	Thickness (mm)	$D_{outside}$ (mm)	D_{inside} (mm)
				F1 (P1 + base)	60	3228	2708
P1	3.5	3228	3107		22		
P2	17.5	3107	2150		20		
				F2 (P2-P3)	100	2150	1920
P3	3.5	2150	1675		20		
				F3 (P3–P4)	75	1675	1420
P4	7.0	1675	1565		18		
P5	3.5	1656	1495		16		
P6	3.5	1495	1425		14		
P7	3.5	1425	1355		12		
P8	3.5	1355	1200		10		
				F4 (P2–P3)	40	1200	1000
Total	45.5						

fixing the strain gauges in position with the proper adhesive. Afterwards, the sensors were cabled and the protective coating was finally applied to protect both the sensors from dust and humidity and the tower steel from corrosion (Fig. 6).

The data acquisition system is composed of a precision instrument for static and dynamic acquisition which includes a scanner with 8 channels. Each channel can be configured independently to accept strain gauge with multiple configurations or thermal couples. Acquired data is processed and filtered using Finite Impulse Response (FIR) to achieve an optimal noise reduction. The system is checked via proprietary software provided with the hardware and runs locally on a laptop which can be accessed remotely. The software also allows for a wide range of sampling frequencies (from 10 to 1000 Hz) and provides a simple way to arm or disarm the sensors. In the current configuration, the bolts were not monitored.

3.2 Results: modal response

The accelerations in different working conditions were extracted in different times throughout 1 year of service life. To perform modal identification, the Operational Modal Analysis (OMA) technique [31] could be used where the dynamic excitation was unknown. The main part of the dynamic load typically consists of artificial and/or natural sources of vibration present around the structure. Since the input is assumed as unknown, only the response of the structure could be analysed (modal output-only analysis). The analysis of the acquired data is based on the study of the Power Spectrum function, Crosspower-spectrum of two signals, one of which is taken as a reference between all the collected data sets. This function can be decomposed into series as a combination of the frequency modal parameters, damping and deformations.

In detail, the modal parameters have been extracted for:

- wk1, wind turbine in case of wind under 3 m/s. In this case, the rotor was not activated;
- wk2, wind turbine in case of rotor working with low velocity (about 20 rpm);
- wk3, wind turbine at the condition used to guarantee optimal energy production (32 rpm).

The three working conditions have been repeated three times during different external temperatures (winter and summer) finding no sensible differences. Table 2 lists the results associated with the turbine.

The study of the dynamic behaviour of the wind tower showed that the fundamental frequency of about 0.6 Hz is very close to the working frequency of the rotor at 32 rpm. This fact exposes the structures to resonance phenomena which can be triggered and amplified by even small

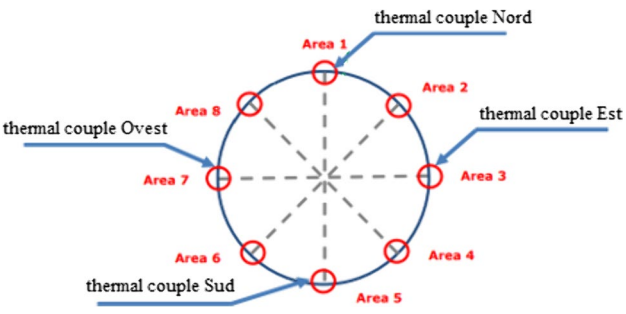

Fig. 8 Position of the strain-gauges and thermal couples in the cross-section

variations of initial conditions: little imbalances in the masses and angles of attack of the blades, misalignment in the control bodies of the nacelle orientation, dissymmetry in the structure of the towers, asymmetries in the interface between foundations and structures, peculiar turbulence phenomena due to the orography or the presence of other structures for particular wind directions, differential settlements of the foundation plane. Furthermore, for security reasons the lock of the system is activated when the rotor come close to 32 rpm. The first and the second frequencies are identical in value and are represented by the typical deformed shape of an inverted pendulum with a rotational mode of the tower head that follows an elliptical trajectory on the horizontal plane. The third and the fourth modal shapes are the ones represented by the higher mode of an inverted pendulum.

3.3 Results: normal stresses

A one-year experimental campaign was carried out by continuously monitoring the tower. It is important to notice that, since the strain-gauges were mounted on an already working tower, the self-weight and the weight of the rotor could not be measured with the proposed system, therefore only the strains generated at a specific operating condition are considered in the following [32]; in other words, the strains are related to the time-varying response under external wind action. For this reason, it is important to understand that when the wind velocity is low and the turbine is in an idle position, the measurement system does not give any value. Consequently, in these conditions, the whole measurement system has been adequately calibrated. The maximum axial force due to the nacelle and tower self-weight is 712.6 kN, which generates a normal stress of 2.65 MPa on the monitored section, considered as a uniform compressive stress on the shell. The direct results extrapolated from the campaign were the curves that relate strain in one main direction, ε_z, over time. The complete measuring system used together with the integrated system in the nacelle allowed correlating strain measurement with (i) wind velocity; (ii) hub position; (iii) rpm of the rotor. For the damage evaluation, it is convenient to refer to the results as a variation of stresses, $\Delta\sigma_z$ by using Hooke's expression:

$$\Delta\sigma_z = E \cdot \Delta\varepsilon_z \tag{3}$$

where $\Delta\varepsilon_z$ and $\Delta\sigma_z$ are the variation of strains and stresses, acting normally to the cross-section, in z direction, and E is the Young modulus of the steel (assumed equal to 210 GPa). The use of a Wheatstone bridge prevented the temperature variation from influencing the stresses; this nonetheless, it was registered thanks to the thermal couples installed. The results shown in the paper are the ones obtained starting from the calibration of the instruments. It should be noted that interruptions due to system malfunctioning, planned maintenance activities and errors in data transmission occurred during the year in question, so no 365-day monitoring was possible.

As an example of the output derived from the monitoring system, Figs. 9 and 10 can be considered, both related to 30 h of continuous monitoring. In the figures the position of the strain gauges is reported together with the variation of stresses in time (for 2 selected channels) and with the rpm of the rotor versus time. The time series are related to 26th April and 4th May 2022, respectively.

The limit of 32 rpm is marked with a red horizontal line. This limit cannot be exceeded by the rotor. Orange vertical lines highlight the range in which the rotor grants the best energy production (28 ÷ 32 rpm). Regardless of the season, once the rotor enters the optimal range, the measured $\Delta\sigma_z$ increases immediately. Hence, the damage index is expected to noticeably increase when the turbine works in this velocity range. It should be noted that sometimes curve *c* shows rotor velocity equal to zero: this can be related to a drop of the wind velocity (which is lower than 3 m/s and hence not sufficient to ensure power production) or to a stop of the rotor for maintenance or safety reasons. An interesting comparison can be made between the measured wind velocities and the rpm of the rotor, as shown in Fig. 11 for the considered 30 + 30 h registrations, both obtained from the SCADA system of the turbine.

In the wind velocity part, the full registration data is proposed together with the moving average every 10 min. With the black horizontal line, the mean value of the total registration is highlighted. For the considered registration it could be observed that the shape of the rotor rpm is exactly the one related to the moving average of the wind: as discussed, when the wind drops to zero, the rpm follows. Interestingly,

Table 2 Modal properties of the turbine under different working conditions

Working condition	Rotor speed (rpm)	I–II mode		III–IV mode	
		Frequency (Hz)	Damping (%)	Frequency (Hz)	Damping (%)
wk1	0.0	0.61	3.1	3.9	1.2
wk2	20.0	0.60	3.1	3.9	3.2
wk3	32.0 (0.55 Hz)	0.55	2.9	4.0	3.2

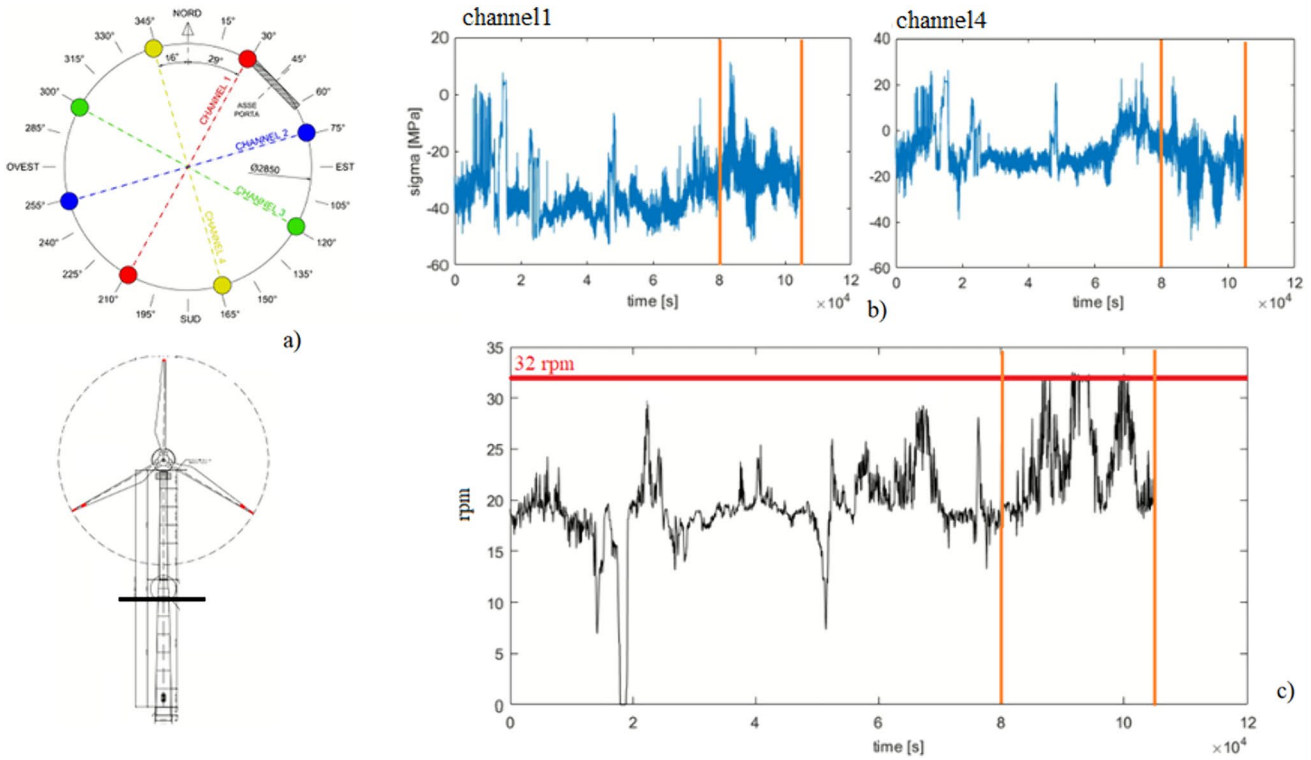

Fig. 9 Typical output for 30 h monitoring (26th April 2022): **a** position of the channels, **b** stresses vs time, for ch1 and ch4, and **c** rpm vs time (red line represents 32 rpm value). The part between vertical lines corresponds to the area in which the 32 rpm value was reached (colour figure online)

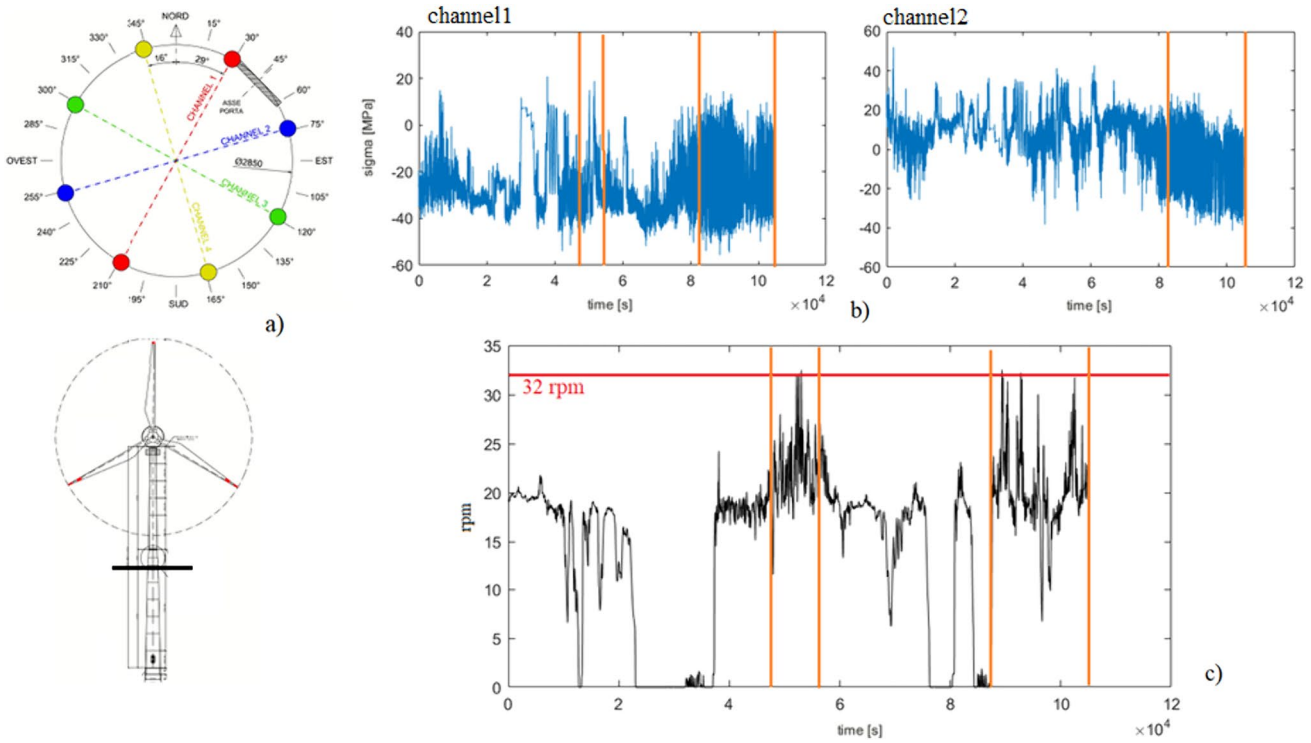

Fig. 10 Typical output for 30 h monitoring (4th May 2022): **a** position of the channels, **b** stresses vs time, for ch1 and ch2, and **c** rpm vs time (red line represents 32 rpm value). The part between vertical lines corresponds to the area in which the 32 rpm value was reached (colour figure online)

the same does not occur when the wind velocity increases and this is due to the rotor limitation. Energy production is hence greatly reduced due to this limited choice.

To further explore the resonance problem, during a windy day (30th April 2022) the tower was made to work at its limit for 20 h. In Fig. 12 the output in terms of maximum stresses and rpm is shown. A great increase in the monitored stresses can be observed with respect to the initial part of the registration for which the stress level is comparable to the ones displayed in the previous figures. The phenomenon is directly linked to the initiation of the structural resonance, which results in a dangerous state of stress for the tower. A typical resonance effect is an unconditional increase in the displacements in time with limited effect by the structural damping. The limit of 32 rpm is hence necessary to guarantee the tower's safety and cannot be overpassed, not only with respect to the fatigue life but also regarding the maximum admissible stresses themselves.

4 Considerations about fatigue

As discussed in the second section, the first step for the damage estimation of a component is the use of a refined procedure to count the stress ranges. For this research, the *Rainflow* counting procedure was used. The complete procedure was implemented inside MATLAB. The output of the counting procedure is composed of two different graphs: one related to the S–N spectra for the selected range of time and the other one related to the occurrence for each stress range. Figure 13 is an example of this, referring to the previous Figs. 9 and 10.

During the 30 h monitoring in April, the considered turbine underwent a greater stress variation with respect to May. On the contrary, in May stresses were more widely distributed in time. Indeed, Fig. 13 shows that the histogram of May is wider and smaller. Finally, the same procedure is applied to the recorded stresses of 30th April 2022, presented in Fig. 14. The resonance produces a different stress distribution, resulting in great stress variation values.

Once the number of occurrences is detected, Eqs. (1) and (2) can be applied; the detail class must be suitably selected in accordance with EC3-1-9 [33]. To understand the influence of the resonance on the stresses and hence on the damage index, Table 3 is proposed with the ratio between DEL and the detailed class (Eq. 2b) and the maximum and the minimum tensions (s_{max} and s_{min}) recorded in the channel with the higher DEL. The table also displays the maximum wind velocity and the higher stress variation (Δs_m). For the sake of shortness, the values in Table 3 only refer to some selected days of the year in question. Finally, 32 rpm working conditions have been highlighted via a grey background.

In the table the whole stress range has been considered, i.e. the curves of the monitored stresses were considered for their full length without any modification. The component

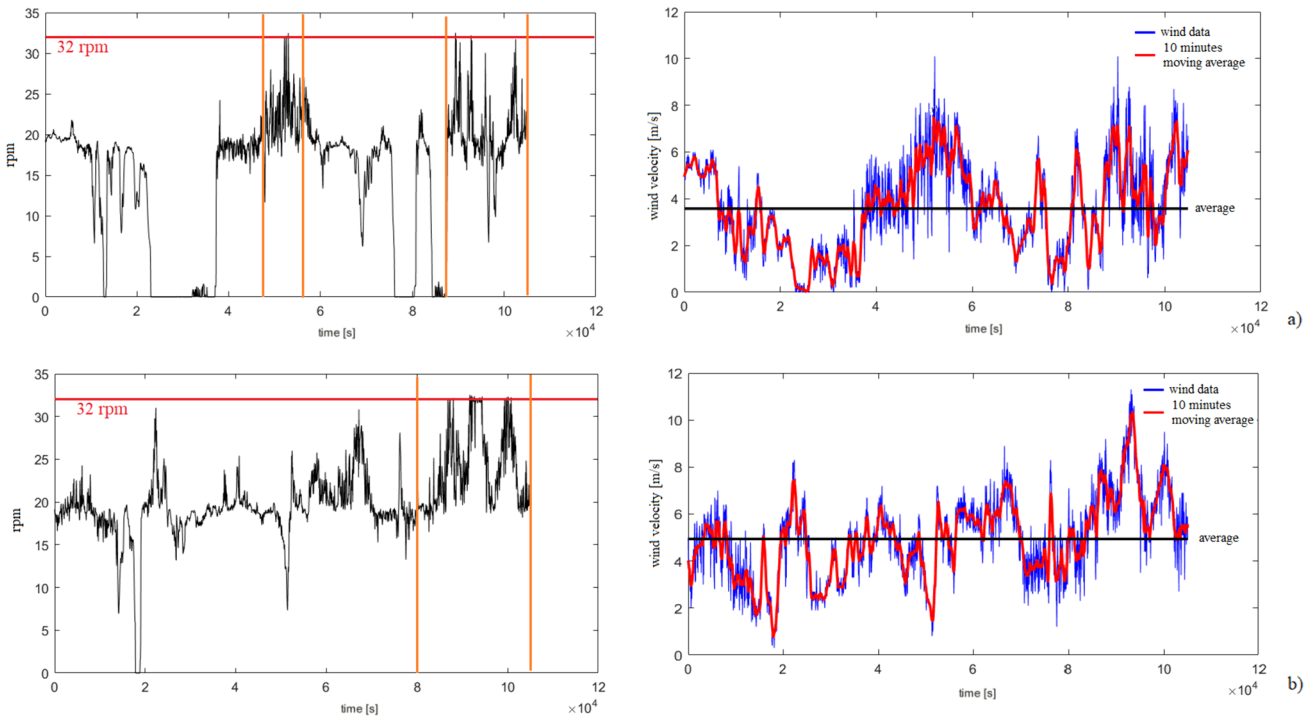

Fig. 11 Rpm and wind vs time: **a** 26th April and **b** 4th May 2022

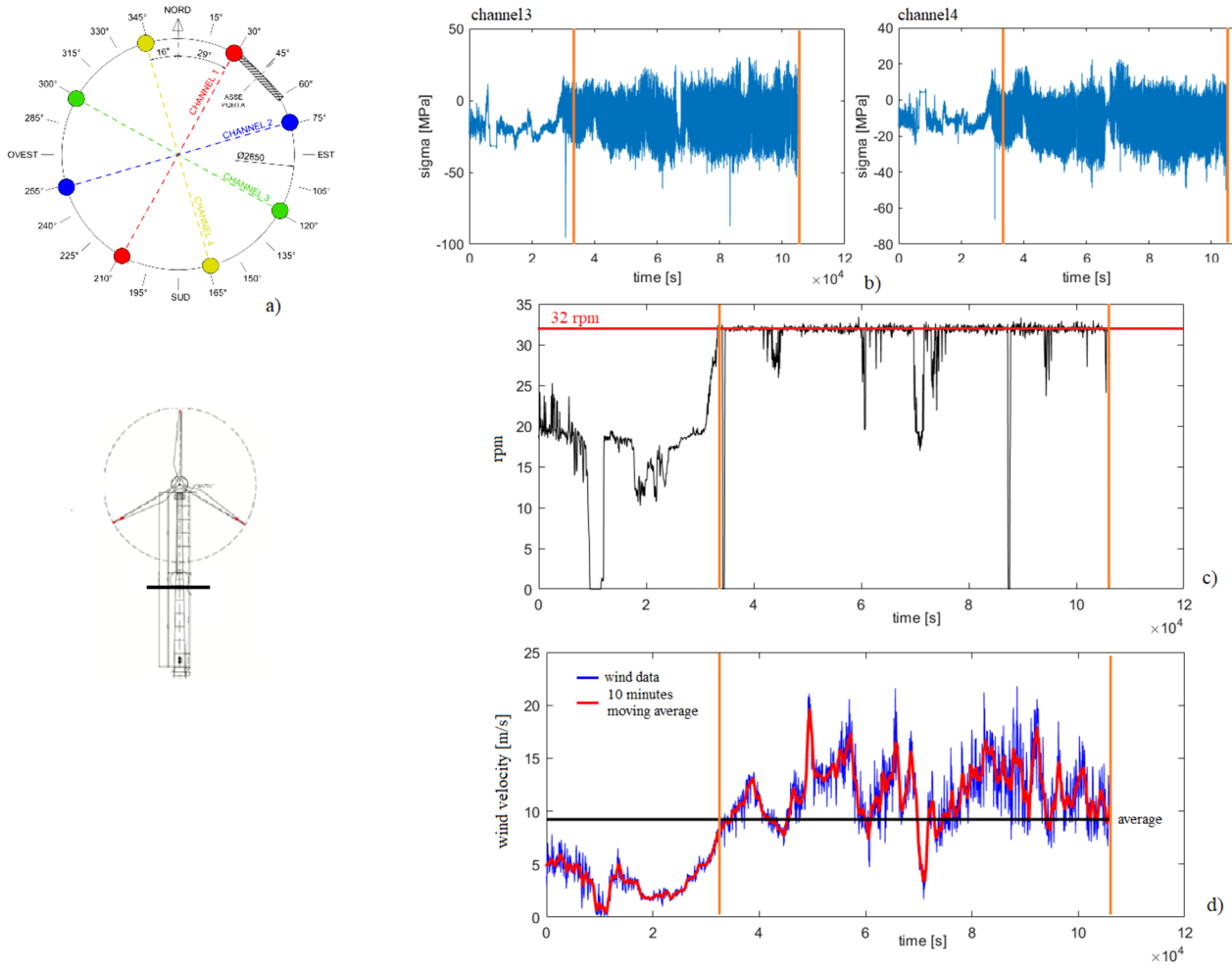

Fig. 12 Output associated with the tower in resonance for about 20 h: **a** position of the channels, **b** stresses vs time, for ch3 and ch4, **c** rpm vs time (red line represents 32 rpm value), and **d** wind velocity. The part between vertical lines corresponds to the area in which the 32 rpm value was reached (colour figure online)

safety associated with the normal working condition, first seven rows, when 32 rpm is reached occasionally, is in average equal to 0.0295. On the contrary, in highly windy days, where the working condition was always associated with 32 rpm, the ratio increases up to 0.0828 (almost 3 times greater than normal days).

The Damage index, D_d, of the turbine can be evaluated after 1 year considering that:

- when the wind velocity was lower than a threshold value (3 m/s), the rotor was not activated (i.e. no energy production) and hence no data about the stress variation have been obtained on those days (Damage is considered nil);
- as previously discussed, throughout the year the monitoring system sometimes needed to be reactivated due to maintenance or magnetic interference associated with the turbine itself;
- all the stresses registered in different days have been collected in one very large file and then the damage index has been evaluated. To obtain a comparison between normal working conditions and extreme working conditions, the days in which the rotor was made to work for different hours in a row at around 32 rpm rotor velocity have been collected in a separate file from the other days (which represents around the 5% of the total monitored hours).

In the considered year of monitoring, for normal operation condition 2.16×10^7 s have been monitored with a cumulated damage equal to $D_n = 5.28 \times 10^{-3}$. A similar damage level ($D_r = 5.13 \times 10^{-3}$) was reached in *resonance* condition, but only with 1.73×10^6 s of monitoring activity. The correct projection of the stresses throughout the years should contemplate the wind distribution of the site by statistically considering wind velocities in time. The most unfavorable estimation of the damage can be made by linearly

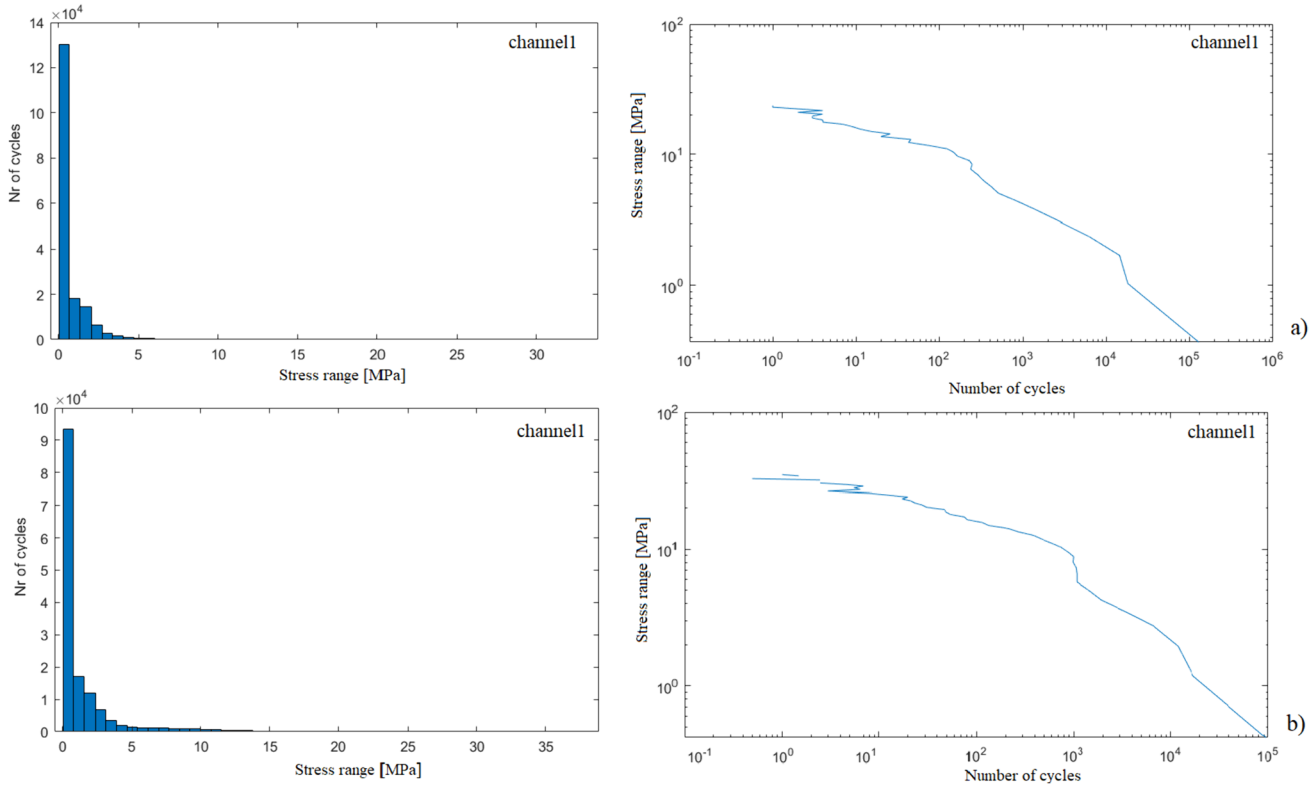

Fig. 13 Output of the Rainflow procedure from the total time series: **a** 26th April and **b** 4th May 2022

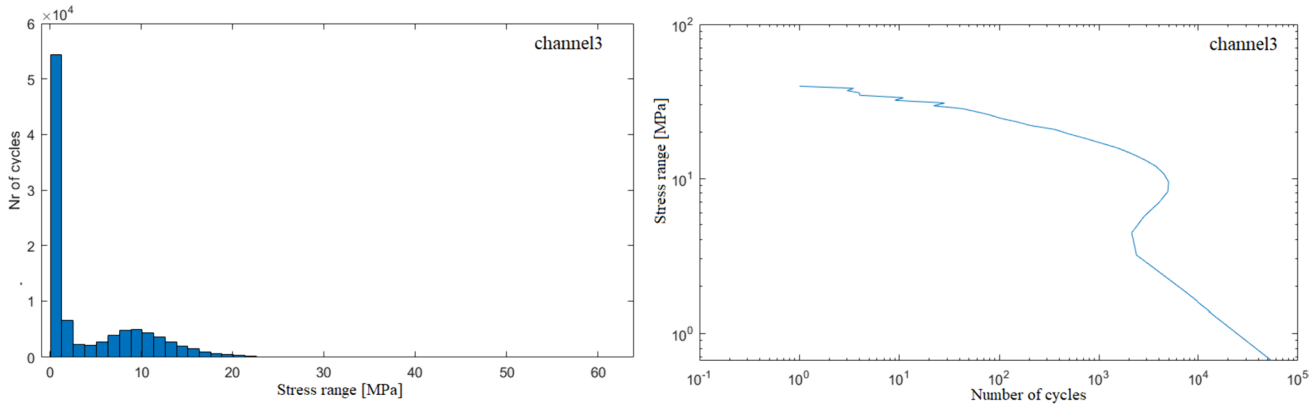

Fig. 14 Output of the rainflow procedure from the total time series: 30th April 2022

considering the project of the monitored year throughout the time, as done in Ref. [24]:

$$\text{Lifetime(N.C.)} = \frac{\text{Time(year)}}{D_n} = \frac{2.16 \cdot 10^7}{(3600 \cdot 24 \cdot 365)} \frac{1}{5.28 \cdot 10^{-3}} = 130\,\text{years} \tag{4a}$$

$$\text{Lifetime(resonance)} = Z\frac{\text{Time(year)}}{D_r} = \frac{1.73 \cdot 10^6}{(3600 \cdot 24 \cdot 365)} \frac{1}{5.14 \cdot 10^{-3}} = 11\,\text{years} \tag{4b}$$

Due to the resonance problem, assuming the turbine operates constantly at 32 rpm, the fatigue limit is reached after 11 years. On the contrary, in the case of normal working conditions, the maximum fatigue damage index can be reached after the 20 years prescribed by the Code. This

Table 3 DEL evaluation for some selected days in a 1-year monitoring range

Year 2022	Channel	$\Delta\sigma_m$ (MPa)	Equation (2b) (–)	σ_{max} (MPa)	σ_{min} (MPa)	Wind velocity (max moving average) (m/s)
19th April	2	31.94	0.0298	44.80	−46.61	8.3
26th April (Fig. 10)	1	34.05	0.0277	61.12	−27.43	10.2
4th May (Fig. 11)	3	37.99	0.0358	52.53	−41.93	9.4
21th May	3	32.36	0.0410	60.00	−17.14	10.7
28th June	4	35.15	0.0194	65.53	−18.50	7.8
6th July	2	41.55	0.0331	45.22	−49.55	9.5
2th August	2	30.25	0.0295	32.25	−41.25	8.8
30th April (Fig. 13)	3	57.99	0.0828	14.34	−123.08	19.8
12th May	3	54.51	0.0789	69.22	−78.24	18.6

suggests that wind turbines with no structural problems can mount an adequate monitoring system to increase their service life. Moreover, it is confirmed that, if the resonance phenomenon is not counterbalanced by imposing a limit on the rotor velocity, the damage exponentially increases, and the service life of the turbine is drastically reduced.

All these considerations are only about the fatigue life estimation and do not consider the deterioration of other components in time due to different phenomena. The results can be extended to other critical components, like bolts, which have not been monitored.

5 Concluding remarks

Pollution, the extensive use of fuel in the last century, the pandemic situation due to COVID-19 and the recent East Europe war highlighted how the world is reaching a non-returning point on the energetic crisis. Climate change and environmental degradation are a huge threat and practical actions cannot be postponed any longer. Therefore, it is crucial that each European country moves towards renewable energy production, for instance via wind turbines—which, despite helping resolve the aforementioned issues, offer no optimal solution. On the one hand, the benefit of renewable energy production is there, but on the other hand the waste steel from the turbines after their service life is over remains an issue. There is still a non-negligible unsolved problem: how can we increase the operational service life of steel wind turbines? The first step is to understand if the design assumption which prescribes dismantling the wind turbine components every 20 years is realistic or too strict. On the contrary, some phenomena such as resonance can drastically decrease the service life of such a structure.

This paper presents the results of a complex monitoring system applied to an existing steel tubular wind tower located in Italy. To increase the safety level of the structure and understand the stress distribution on the tower a combination of strain gauges, thermal couples and accelerometers were installed along it. The turbine is approximately 45 m high (hub height) and it is subjected to a resonance problem which led producers to limit rotor velocities. It has been observed that when 32 rpm are reached, the tower entails abnormal oscillation.

Firstly, an extensive campaign was performed via suitably located accelerometers, which highlighted the resonance problem of the structure. Then, the monitoring system was used to correlate the maximum stress and the consequent damage (D_d) indexes with the velocity of both the rotor and the wind.

It has been shown that, in normal working conditions, the tower does not suffer from fatigue problems and hence the design life can be extended well beyond the usual 20 years. On the contrary, when the rotor velocity touches around 32 rpm, the stress variation greatly increases. If the turbine (ideally) works close to this rotor velocity, the service life is limited to about 11 years. These results showed two main general conclusions:

- a complete structural health monitoring system, like the one discussed herein, brings precise information to the real-time state of stress of the turbine components. The procedure should be used to extend the monitoring system to other critical components like bolts or anchors, on different flanges of the tower, to have a complete view of the real state of the tower;
- the considerations about the remaining fatigue life became more accurate as the monitoring time increased;
- by monitoring the accelerations and hence the modal characteristic, any changes in modal shape or frequency due to damage could be appreciated in real time.

It should be concluded that with such a monitoring system, it is possible to understand whether the turbine undergoes any local or global structural problems.

The quite huge costs associated with the installation of the system (which can be reduced if the tower is not erected) and the data processing can be counterbalanced by extending the service life—and hence by extending energy production.

Funding Open access funding provided by Politecnico di Milano within the CRUI-CARE Agreement.

Data availability The data used for this study are highly sensitive. For additional information contact directly the corresponding Author.

Declarations

Conflict of interest The authors declare that they have no financial or personal conflict of interest that could have influenced the results of the presented work.

References

1. Maglio M (2022) Visions of cities beyond the Green Deal: from imagination to reality. J Urban Regen Renew 15(2):176–192
2. Kenneth B, Marten O (2022) COVID-19, green deal and recovery plan permanently change emissions and prices in EU ETS Phase IV. Nat Commun. https://doi.org/10.1038/s41467-022-28398-2
3. Sakka EG, Bilionis D, Vamvatsikos D, Gantes C (2020) Onshore wind farm siting prioritization based on investment profitability for Greece. Renewable Energy 146:3827–2839. https://doi.org/10.1016/j.renene.2019.08.020
4. Zhang S, Chen W (2022) Assessing the energy transition in China towards carbon neutrality with a probabilistic framework. Nat Commun. https://doi.org/10.1038/s41467-021-27671-0
5. Mishnaevsky Jr M, Branner K, Petersen HN, Beauson J, McGugan M, Sorensen BF (2017) Materials for wind turbines blades: an overview. Materials 10:1285. https://doi.org/10.3390/ma10111285
6. Akan AP, Akan AE (2022) Evaluation of feasibility analyses for different hub heights of a wind turbine. J Energy Syst 6(1):97–107. https://doi.org/10.30521/jes.955100
7. Mohammadi MRS, Richter C, Park D, Carlos R, Feldmann M (2018) Steel hybrid onshore wind towers installed with minimal effort: development of lifting process. Wind Energy 41(4):335–352. https://doi.org/10.1177/0309524X18777331
8. Gkantou M, Rebelo C, Baniotopoulos C (2020) Life cycle assessment of tall onshore hybrid steel wind turbine towers. Energies 13(15):3950. https://doi.org/10.3390/en13153950
9. GWEC (2021) Global wind report—annual market update 2021. www.gwec.net. Accessed 2021
10. Mar AM, Jose MA, Felipe PAR (2019) Wind turbine tower collapse due to flange failure: FEM and DOE analyses. Eng Fail Anal 104:22–39. https://doi.org/10.1016/j.engfailanal.2019.06.045
11. Matos R, Shah Mohammadi MR, Rebelo C (2018) A year-long monitoring of preloaded free-maintenance bolts—estimation of preload loss on BobTail bolts. Renewable Energy 116:123–135. https://doi.org/10.1016/j.renene.2017.05.092
12. Ma Y, Martinez-Vazquez P, Baniotopoulos C (2019) Wind turbine tower collapse cases: a historical overview. Proc Inst Civil Eng Struct Build 172(8):547–555. https://doi.org/10.1680/jstbu.17.00167
13. Bernuzzi C, Crespi P, Montuori R, Nastri E, Stochino F, Simoncelli M, Zucca M (2021) Resonance problem of steel wind turbines: problems and solutions. Structures 32:65–75. https://doi.org/10.1016/j.istruc.2021.02.053
14. IEC-61400. Wind energy generation systems—part 1: design requirements. International standard IEC. 4.0 edn, 2019-02
15. EN1991 (2004) Eurocode 1: actions on structures—part 1–4: general actions—wind actions
16. Patil BP, Thakare HR (2015) Computational fluid dynamics analysis of wind turbine blade at various angles of attack and different reynolds number. Proc Eng 127:1363–1369. https://doi.org/10.1016/j.proeng.2015.11.495
17. Diaz O, Suarez LE (2014) Seismic analysis of wind turbines. Earthq Spectra 30(2):743–765. https://doi.org/10.1193/123011EQS316M
18. Nuta E, Christopoulos C, Packer JA (2011) Methodology for seismic risk assessment for tubular steel wind turbine towers: application to Canadian seismic environment. Can J Civ Eng 38(3):293–304. https://doi.org/10.1139/L11-002
19. DNVGL-ST-0126 (2018) Supporting strucutures for wind turbines, July 2018
20. Larsen K (2009) Recycling wind turbine blades. Renewable Energy Focus 9(7):70–73. https://doi.org/10.1016/S1755-0084(09)70045-6
21. Oliveira G, Magalhaes F, Cunha A, Caetano E (2016) Development and implementation of a continuous dynamic monitoring system in a wind turbine. J Civil Struct Health Monitor 6:343–353. https://doi.org/10.1007/s13349-016-0182-7
22. Hu WH, Thons S, Rohrmann RG, Said S, Rucker W (2015) Vibration-based structural health monitoring of a wind turbine system. Part I: resonance phenomenon. Eng Struct 89:260–272. https://doi.org/10.1016/j.engstruct.2014.12.034
23. Benedetti M, Fontanari V, Zonta D (2011) Structural health monitoring of wind towers: remote damage detection using strain sensors. Smart Mater Struct 20(5):055009. https://doi.org/10.1088/0964-1726/20/5/055009
24. Rebelo C, Veljkovic M, Simoes da Silva L, Simoes R, Henriques J (2012) Structural monitoring of a wind turbine steel tower—part I: system description and calibration. Wind Struct 15(4):285–299. https://doi.org/10.12989/was.2012.15.4.285
25. Veljkovic M, Heistermann C (2012) HISTWIN—high-strength tower in steel for wind turbines (contract no, RFSR-CT-2006-00031). RFCS Project, Brussels, Belgium
26. Soyoz S, Hanbay S, Bagirgan B, Ergun O (2021) Long-term vibration-based monitoring and seismic performance assessment of a wind turbine. J Civil Struct Health Monitor 11:117–128. https://doi.org/10.1007/s13349-020-00442-z

27. Li S-Z et al (2023) Damage detection of flange bolts in wind turbine towers using dynamic strain response. J Civil Struct Health Monitor 13:67–81. https://doi.org/10.1007/s13349-022-00622-z
28. EN1993-1-1 (2005) Eurocode 3: design of steel structures—part 1-1: general rules and rules for buildings
29. Bannantine JA, Comer JJ, Handrock JL (1990) Fundamentals of metal fatigue analysis. Prentice-Hall, Englewood Cliffs, NJ
30. Downing SD, Socie DF (1982) Simple rainflow counting algorithms. Int J Fatigue 4:31–40. https://doi.org/10.1016/0142-1123(82)90018-4
31. Peeters B, Karkle P, Pronin M, Van Der Vorst R (2011) Operational modal analysis for in-line flutter assesment during wind tunnel testing. In: IFASD conference proceedings, Paris
32. Millett JCF, Bourne NK, Rosenberg Z (1996) On the analysis of transverse stress gauge data from shock loading experiments. J Phys D Appl Phys 29(9):2466–2472. https://doi.org/10.1088/0022-3727/29/9/035
33. EN1993-1-9 (2009) Eurocode 3: design of steel structures—part 1–9: Fatigue